

Severe Fibronectin-Deposit Renal Glomerular Disease in Mice Lacking Uteroglobin

Zhongjian Zhang, Gopal C. Kundu, Chiun-Jye Yuan,
Jerrold M. Ward, Eric J. Lee, Francesco DeMayo,
Heiner Westphal, Anil B. Mukherjee*

Despite myriads of biological activities ascribed to uteroglobin (UG), a steroid-inducible secreted protein, its physiological functions are unknown. Mice in which the uteroglobin gene was disrupted had severe renal disease that was associated with massive glomerular deposition of predominantly multimeric fibronectin (Fn). The molecular mechanism that normally prevents Fn deposition appears to involve high-affinity binding of UG with Fn to form Fn-UG heteromers that counteract Fn self-aggregation, which is required for abnormal tissue deposition. Thus, UG is essential for maintaining normal renal function in mice, which raises the possibility that an analogous pathogenic mechanism may underlie genetic Fn-deposit human glomerular disease.

Blastokinin (1) or UG (2) is a steroid-inducible, evolutionarily conserved, homodimeric secreted protein with many biological activities including the ability to inhibit soluble phospholipase A₂ (sPLA₂) activity, inflammation, and chemotaxis of neutrophils and monocytes (3). UG binds with high affinity to specific putative receptor sites on several cell types (4, 5) and through this pathway inhibits cellular invasion of the extracellular matrix (4). Although UG was first discovered in the rabbit uterus, it is also expressed in numerous extrauterine tissues (6) and has been detected in the blood (7) and urine (8), but it is not expressed in the kidneys (6). Depending on the tissue of origin or its interaction with xenobiotics (for example, progesterone, retinol, and polychlorinated biphenyls), UG has been given several names (5, 9). The tissue-specific expression of the gene encoding UG is regulated by steroid hormones (3). The nonsteroid hormone prolactin further enhances steroid-induced UG gene expression (10), and the proinflammatory cytokine interferon- γ stimulates UG production in the murine lungs (11), suggesting a potential role of UG in the regulation of immunological inflammatory processes. In addition, the inhibition of the recognition of embryonic and sperm

antigens by lymphocytes and the inhibition of chemotactic peptide (formyl-Met-Leu-Phe)-induced monocyte and neutrophil chemotaxis by UG suggest that UG has immunomodulatory properties (12). Human UG (hUG) is encoded by a single-copy gene on chromosome 11q12.3-13.1 (13), a region to which a number of candidate disease genes have been mapped. Despite more than three decades of intense investigations, which uncovered several important biological properties of UG *in vitro*, the *in vivo* functions, until now, remained obscure.

To understand the physiological roles of UG, we generated UG-deficient (UG^{-/-}) mice by gene-targeting in embryonic stem (ES) cells. The UG gene from the 129/SVJ mouse strain (14) was used in the gene-targeting construct (Fig. 1A) that was introduced into ES R1 cells (15) by electroporation. Gancyclovir and G-418 counterselection of the electroporated cells yielded 156 clones. Southern (DNA) blot analysis identified a 5.1-kb Hind III fragment of the wild-type UG allele and an additional 8.2-kb Hind III fragment resulting from homologous recombination in three out of the 156 clones analyzed (Fig. 1B). These ES R1 clones were injected into C57BL/6 blastocysts (16), generating two different lines of mice, each of which descended from an independent chimeric founder. Heterozygous (UG^{+/-}) offspring carrying the targeted UG gene locus were mated, and the genotypes of the progeny were analyzed by polymerase chain reaction (PCR) (Fig. 1C) and Southern blot analyses (Fig. 1D).

We tested the UG gene-targeted mice for expression of UG mRNA and UG protein in several organs including the lungs. Using reverse transcription-PCR (RT-PCR) (17), we detected UG mRNA from the lungs of UG^{+/+} and UG^{+/-} but not of

UG^{-/-} mice (Fig. 1E). Immunoblot analyses (18) of UG protein in the lungs yielded corroborative results (Fig. 1F). Histopathological analyses (19) of the lungs of UG^{-/-} mice lacked UG-specific immunostaining in bronchiolar epithelial cells (Fig. 1G). The prostate and the uteri of UG^{-/-} but not of UG^{+/+} and UG^{+/-} mice lacked UG mRNA and protein.

Of the 179 mice born to crosses of UG^{+/-} mice, 46 (26%) were UG^{+/+}, 90 (50%) were UG^{+/-}, and 43 (24%) were UG^{-/-}, indicating that the disrupted UG gene locus is inherited in a Mendelian fashion and that UG^{+/+}, UG^{+/-}, and UG^{-/-} mice were equally viable at birth. UG^{-/-} mice developed a progressive illness characterized by heavy proteinuria and hypocalcemia associated with profound weight loss. Histopathological examination (19) of affected UG^{-/-} animals revealed a fulminant renal glomerular disease (Fig. 2). Compared with the glomeruli of the UG^{+/+} mice, those of UG^{-/-} mice were hypocellular and had massive eosinophilic proteinaceous deposits. Heterozygotes had a milder form of the renal disease observed in UG^{-/-} mice. The majority of the UG^{-/-} mice that initially appeared to be healthy had focal glomerular deposits at 2 months of age. However, at about 10 months of age (late onset disease) many of these apparently healthy mice had extreme cachexia similar to that of the mice dying at 4 to 5 weeks of age (early onset disease). The histopathology of the kidneys of mice with late onset disease showed not only severe glomerulopathy as with early onset disease but also had marked fibrosis of the renal parenchyma and tubular hyperplasia (Fig. 2). Although the predominant pathology in the UG^{-/-} mice was found in the kidneys, histopathological studies also uncovered focal areas of necrosis in the pancreas.

Because reactive amyloidosis may occur in response to inflammation and because UG has immunomodulatory and antiinflammatory properties, we stained kidney sections from UG^{+/+} and UG^{-/-} mice with Congo red and examined them under polarized light. Amyloid proteins yield a positive birefringence in this test; however, the glomeruli of UG-null mice were negative. Immunofluorescence studies for the presence of immunoglobulin A (IgA), IgG, or IgM immunocomplexes in the glomeruli of UG^{-/-} mice and immunohistochemical analyses for the presence of major amyloid proteins were also negative. Thus, the glomerular deposits of UG^{-/-} mice contained neither amyloid proteins nor immunocomplexes.

We examined the kidney deposits of UG^{-/-} mice by transmission electron microscopy (20). These deposits contained primarily two types of fibrillar structures: one type of long and striated fibrils, which

Z. Zhang, G. C. Kundu, C.-J. Yuan, A. B. Mukherjee, Section on Developmental Genetics, Heritable Disorders Branch, National Institute of Child Health and Human Development (NICHD), National Institutes of Health (NIH), Bethesda, MD 20892-1830, USA.

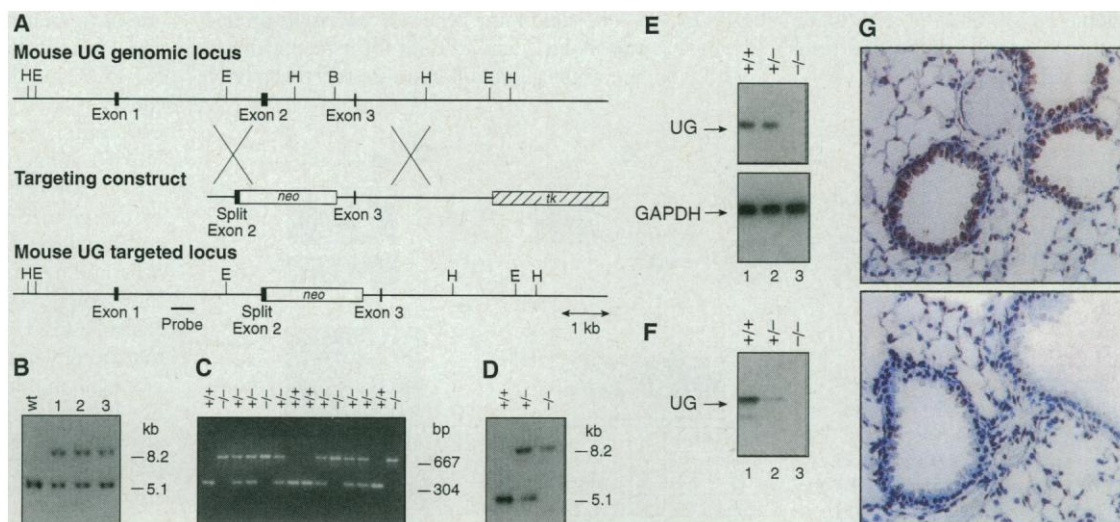
J. M. Ward, Veterinary and Tumor Pathology Section, Office of Laboratory Animal Science, National Cancer Institute, Frederick, MD 21702-1201, USA.

E. J. Lee and H. Westphal, Laboratory of Mammalian Genetics and Development, NICHD, NIH, Bethesda, MD 20892-1830, USA.

F. DeMayo, Department of Cell Biology, Baylor College of Medicine, Houston, TX 77030, USA.

*To whom correspondence should be addressed: E-mail: mukherja@cc1.nichd.nih.gov

Fig. 1. Targeting of the UG locus. **(A)** Diagram of the UG gene locus, targeting construct, and resulting UG targeted locus. B, Bam HI; E, Eco RI; H, Hind III. **(B)** Southern blot analyses of the targeted ES R1 cell clones; wt, wild type. **(C)** Representative PCR analyses of genomic DNA from tail biopsies of offspring. The genotypes and their corresponding PCR products are as follows: UG^{+/+}, 304 base pairs (bp); UG^{+/-}, 304 and 667 bp; and UG^{-/-}, 667 bp. **(D)** Southern blot of mouse tail genomic DNA. **(E)** RT-PCR analyses of total RNA extracted from the lung tissues of littermates with UG^{+/+}, UG^{+/-}, and UG^{-/-} genotypes. A 273-bp RT-PCR product was detectable in the lungs of UG^{+/+} and UG^{+/-} mice but lacking from those of UG^{-/-} mice. **(F)** Protein immunoblot analysis. Proteins (30 μg of each) from lung lysates were resolved by electrophoresis on 4 to 20% gradient SDS-polyacrylamide gels under nonreducing conditions and immunoblotted with anti-UG. **(G)**



Immunohistochemical localization of UG in bronchiolar epithelial cells. The dark staining over the bronchiolar epithelial cells of a UG^{+/+} mouse (upper panel) indicates UG immunoreactivity. Note the absence of immunoreactivity in UG^{-/-} mouse lungs (lower panel). Methods are described in (17-19, 31). Magnification ~×100.

were relatively infrequent, and another type of short and diffuse fibrils, which were more abundant (Fig. 2, E and F). Because extracellular matrix (ECM) proteins, such as collagen and fibronectin, produce similar fibrillar structures, the glomerular deposits in UG^{-/-} mice may contain these proteins. We analyzed the glomerular deposits by immunofluores-

cence (21) using antibodies to murine Fn (anti-Fn). Whereas Fn-specific immunofluorescence in the renal glomeruli of wild-type mice was virtually undetectable (Fig. 2G), that in the glomeruli of UG^{-/-} littermates was intense (Fig. 2H). When Masson's trichrome staining was used, the glomeruli of UG^{+/+} mice were negative (Fig. 2I) and

those of UG^{-/-} (Fig. 2J) mice were positive, suggesting the presence of collagen in the glomerular deposits. Immunofluorescence, with antibodies specific for collagen I and collagen III, confirmed these results. Because Fn is known to interact with other ECM proteins, we also tested for the presence of laminin, vitronectin, and osteopontin in the

those of UG^{-/-} (Fig. 2J) mice were positive, suggesting the presence of collagen in the glomerular deposits. Immunofluorescence, with antibodies specific for collagen I and collagen III, confirmed these results. Because Fn is known to interact with other ECM proteins, we also tested for the presence of laminin, vitronectin, and osteopontin in the

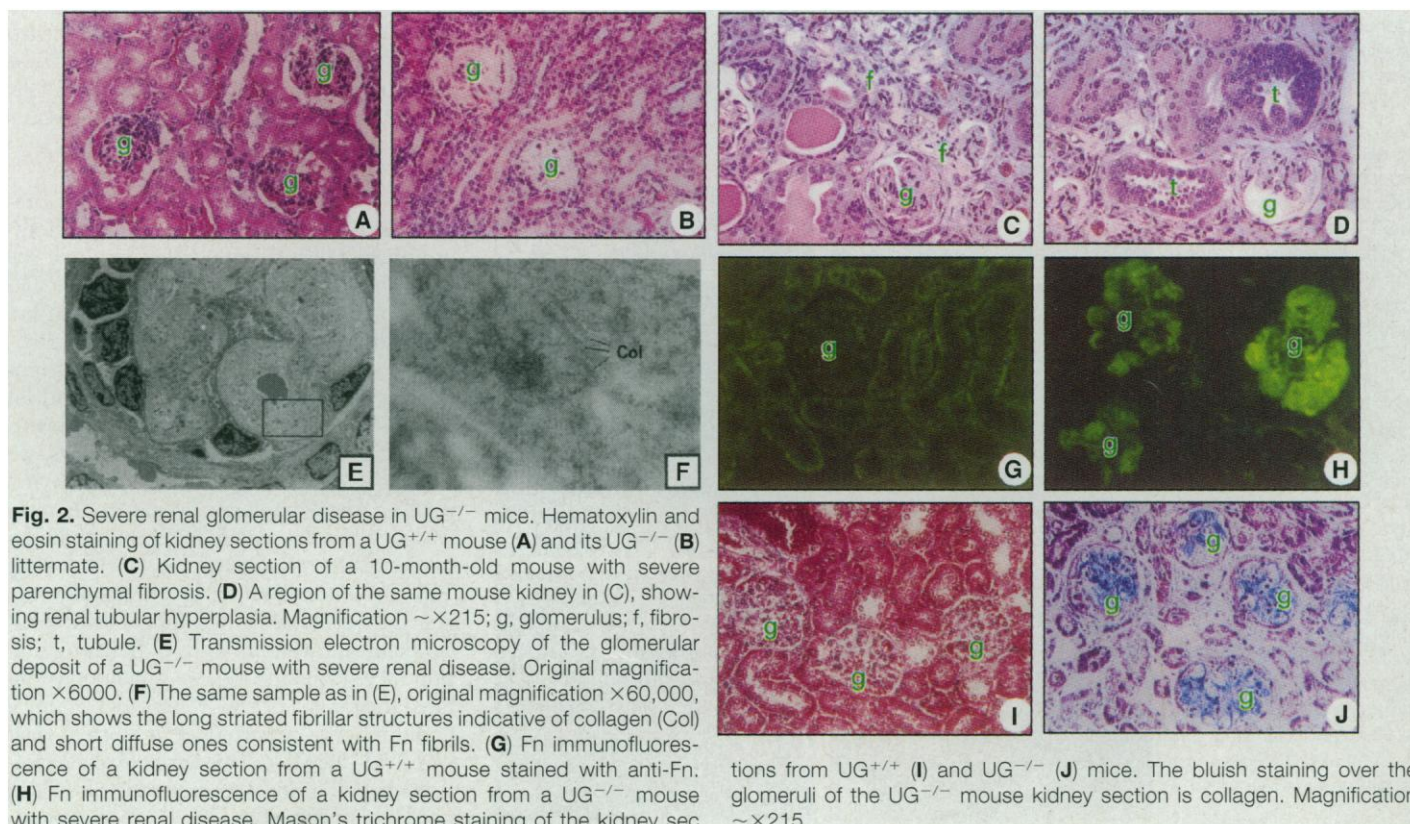


Fig. 2. Severe renal glomerular disease in UG^{-/-} mice. Hematoxylin and eosin staining of kidney sections from a UG^{+/+} mouse **(A)** and its UG^{-/-} **(B)** littermate. **(C)** Kidney section of a 10-month-old mouse with severe parenchymal fibrosis. **(D)** A region of the same mouse kidney in **(C)**, showing renal tubular hyperplasia. Magnification ~×215; g, glomerulus; f, fibrosis; t, tubule. **(E)** Transmission electron microscopy of the glomerular deposit of a UG^{-/-} mouse with severe renal disease. Original magnification ×6000. **(F)** The same sample as in **(E)**, original magnification ×60,000, which shows the long striated fibrillar structures indicative of collagen (Col) and short diffuse ones consistent with Fn fibrils. **(G)** Fn immunofluorescence of a kidney section from a UG^{+/+} mouse stained with anti-Fn. **(H)** Fn immunofluorescence of a kidney section from a UG^{-/-} mouse with severe renal disease. Masson's trichrome staining of the kidney sec-

tions from UG^{+/+} **(I)** and UG^{-/-} **(J)** mice. The bluish staining over the glomeruli of the UG^{-/-} mouse kidney section is collagen. Magnification ~×215.

glomeruli of UG^{+/+} and UG^{-/-} mice by immunohistochemistry, the results of which were negative.

To determine whether excessive production of Fn could account for its deposition in the renal glomeruli, we assessed the relative

amount of Fn mRNA in the kidneys, lungs, and liver of UG^{-/-} and UG^{+/+} mice by RT-PCR and densitometry. The results indicate that relative amounts of Fn mRNA were essentially identical in both UG^{+/+} and UG^{-/-} animals. Thus, overproduction of Fn mRNA was not a likely cause of Fn deposition in the glomeruli of UG^{-/-} mice. We then compared the Fn protein in the plasma, kidneys, and liver of UG^{-/-} and UG^{+/+} mice by SDS-polyacrylamide gel electrophoresis (SDS-PAGE) under reducing conditions and the protein immunoblotting. In the plasma, kidneys, and liver of wild-type mice, only 220-kD Fn species were detected; whereas the plasma and the liver lysates of UG^{-/-} mice had the 220-kD Fn band, the kidney lysates contained another distinct, covalently linked, multimeric Fn band (Fig. 3A).

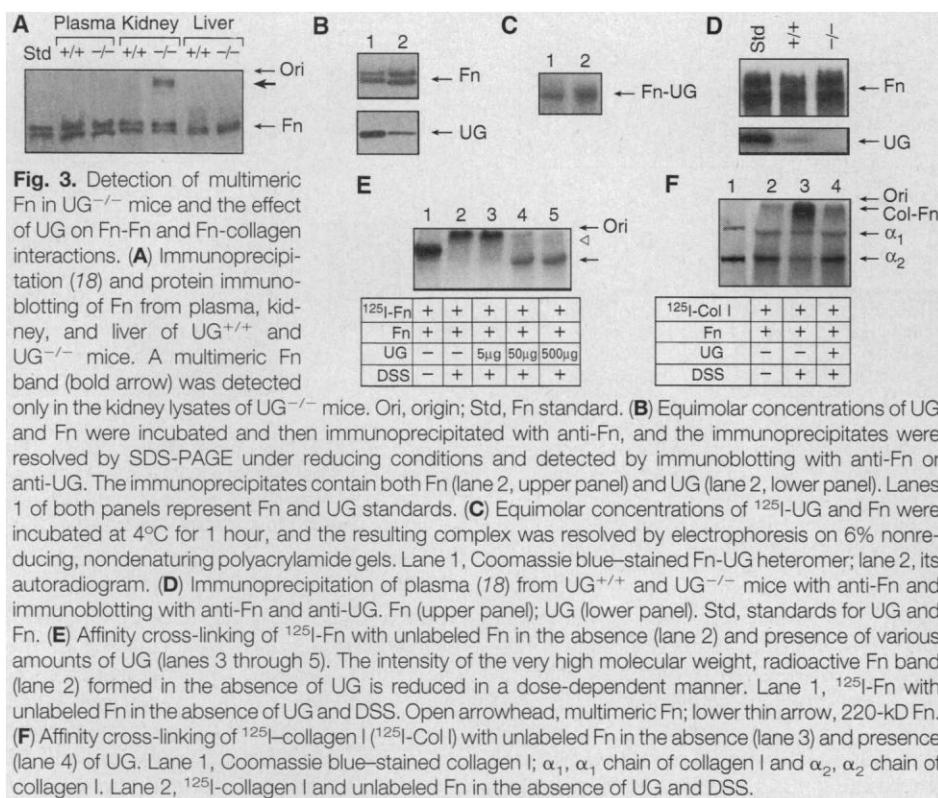
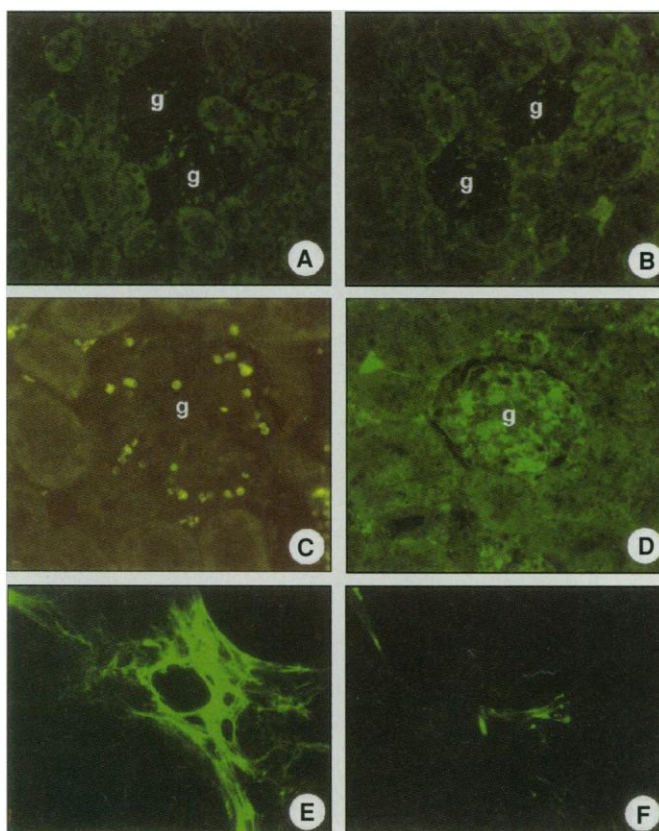


Fig. 4. Inhibition by UG of glomerular Fn deposition, in vitro matrix assembly, and fibrillogenesis. Kidney sections of (A) a wild-type mouse that received a mixture of equimolar concentrations of Fn and UG intravenously; (B) a UG^{+/+} mouse that received the same dose of Fn as in (A) but without UG; (C) an apparently healthy UG^{-/-} mouse that received a mixture of Fn and UG; and (D) a UG^{-/-} mouse that received Fn alone [same dose as in (C)], but without UG. (E) Fn fibrillogenesis by cultured cells (29) grown in medium supplemented with soluble hFn alone. (F) A cell culture identical to the one in (E) that was fed with medium containing a mixture of equimolar concentrations of soluble hFn and UG. Magnification (A to F) $\sim \times 145$; g, glomerulus.



On the basis of current concepts, critical initial steps in Fn matrix assembly and fibrillogenesis, at least on the cell surface, are thought to involve integrin activation and Fn self-aggregation (22). Because UG is a potent inhibitor of sPLA₂ (3), a key enzyme in the inflammatory pathway, the lack of UG in UG^{-/-} mice may contribute to the development of glomerulonephritis, an inflammatory renal disease (23). Moreover, lysophosphatidic acid (LPA), a by-product of PLA₂ hydrolysis of phosphatidic acid, causes integrin activation, Fn matrix assembly, and fibrillogenesis (22). Thus, we measured the specific activity (micromoles per minute per milligram of protein) (24) of serum PLA₂ of UG^{-/-} mice [36 ± 3.3 (SEM)], which was significantly higher ($P < 0.05$, Student's *t* test) than that of UG^{+/+} mice [18 ± 2.8 (SEM)]. These results raised the possibility that higher PLA₂ activity may lead to increased LPA production and consequently promote integrin activation in UG^{-/-} mice.

To further examine how UG may prevent Fn self-assembly, we determined whether it disrupts Fn-Fn interaction in vitro. We incubated equimolar concentrations of UG and Fn, immunoprecipitated with anti-Fn, resolved the immunoprecipitates by SDS-PAGE under reducing conditions, and protein immunoblotted (18) with either anti-Fn or anti-UG. Fn coimmunoprecipitated with UG (Fig. 3B). To confirm these results, we also incubated ¹²⁵I-labeled UG with Fn and resolved the complexes by electrophoresis, using a 6% polyacrylamide gel under nonreducing and nonreducing conditions (Fig. 3C). Detection of an Fn-UG heteromer suggested that soluble Fn may interact with UG. To delineate whether Fn-UG heteromerization takes place in vivo, we immunoprecipitated the plasma of UG^{+/+} and UG^{-/-} mice with anti-Fn, which does not cross-react with UG (Fig. 3D). This antibody coprecipitated both Fn and UG from the plasma of UG^{+/+}, but not from UG^{-/-} mice, suggest-

ing that Fn-UG heteromers are present in the plasma of UG^{+/+} mice.

To determine the specificity and affinity of UG binding to Fn, we incubated ¹²⁵I-labeled Fn with unlabeled Fn in the presence and absence of UG and affinity cross-linked with disuccinimidyl suberate (DSS) (25). In the absence of UG, ¹²⁵I-Fn formed a high molecular weight, radioactive complex with unlabeled Fn, but in the presence of UG the formation of Fn-Fn aggregates was inhibited in a concentration-dependent manner (Fig. 3E). To determine whether there is any difference between the binding affinities of Fn for UG and that of Fn for itself, we did binding experiments in which ¹²⁵I-Fn was incubated with unlabeled Fn (immobilized on multiwell plates) together with various concentrations of UG. In separate experiments, we also did binding studies of ¹²⁵I-Fn with unlabeled immobilized Fn using various concentrations of unlabeled soluble Fn. The Scatchard analyses of the data from both of these binding experiments yielded straight lines with dissociation constants (K_d) of 13 nM for UG binding to Fn and 176 nM for Fn binding to itself. These results suggest that, because of a relatively higher binding affinity of UG for Fn, UG may effectively counteract Fn self-aggregation. We also did affinity cross-linking experiments in which radio iodinated (¹²⁵I)-collagen I was incubated with unlabeled Fn in the absence or presence of UG, as described above for Fn. The results indicate that UG counteracts the formation of high molecular weight ¹²⁵I-collagen-Fn aggregates (Fig. 3F).

To test whether UG protects the renal glomeruli from Fn accumulation, we administered soluble human Fn (hFn) alone or hFn mixed with equimolar concentrations of UG intravenously to UG^{+/+} and to apparently healthy UG^{-/-} littermates (26). The rationale for injecting hFn was to be able to discriminate between endogenous murine Fn and administered hFn. The methods of intravenous administration and immunohistochemical detection of hFn in various tissues have been described (27). After 24 hours, histological sections of the kidneys were examined by immunofluorescence with a monoclonal antibody to hFn. Human Fn immunofluorescence in the glomeruli of wild-type mice injected with either a mixture of hFn and UG (1:1 molar ratio) or with hFn alone was similar (Fig. 4, A and B). However, although the UG^{-/-} mice injected with a mixture of hFn and UG had little hFn-specific immunofluorescence in the glomeruli (Fig. 4C), those receiving hFn alone had higher intensity immunofluorescence (Fig. 4D). Administration of a mixture of hFn and bovine serum albumin (BSA) had no protective effect. To determine whether this protec-

tion could be overcome by injecting larger quantities of hFn in UG^{+/+} mice, we injected 1 mg of hFn per animal daily for three consecutive days (27). Although intravenous administration of hFn to UG^{+/+} mice at lower doses (500 µg per animal) was not effective in causing any appreciable glomerular deposition (Fig. 4A), the administration of higher doses (3 mg per animal) led to a significant accumulation (28). Thus, UG may prevent glomerular Fn deposition, and UG^{+/+} as opposed to UG^{-/-} mice may have a higher threshold for the accumulation of soluble Fn.

To determine whether UG prevents Fn fibrillogenesis and matrix assembly in vitro, we cultured mouse embryonic fibroblasts in medium containing either soluble hFn alone or a mixture of equimolar concentrations of hFn and UG (29). The level of fibrillogenesis in cell cultures treated with hFn alone was much higher (Fig. 4E) compared with those that received a mixture of hFn and UG (Fig. 4F).

Renal diseases are a major cause of human morbidity and mortality, and glomerular diseases are one of the major causes of renal failure. A familial glomerulopathy, characterized by heavy deposition of predominantly fibronectin, has been described (30), although the mechanisms of pathogenesis of this disease remain unclear. The availability of the UG-knockout mouse model may allow us to understand the pathogenic mechanisms of ECM protein-deposit human glomerulopathies in general and the predominantly Fn-deposit hereditary glomerulopathy (30) in particular.

REFERENCES AND NOTES

- R. S. Krishnan and J. C. Daniel Jr., *Science* **158**, 490 (1967).
- H. M. Beier, *Biochim. Biophys. Acta* **160**, 289 (1968).
- S. W. Levin, J. D. Butler, U. K. Schumacher, P. D. Weightman, A. B. Mukherjee, *Life Sci.* **38**, 1813 (1986); L. Miele, E. Cordella-Miele, A. Facchiano, A. B. Mukherjee, *Nature* **335**, 726 (1988); L. Miele, E. Cordella-Miele, A. B. Mukherjee, *Endocr. Rev.* **8**, 474 (1987); L. Miele et al., *J. Endocrinol. Invest.* **17**, 679 (1994).
- G. C. Kundu, G. Mantle, L. Miele, E. Cordella-Miele, A. B. Mukherjee, *Proc. Natl. Acad. Sci. U.S.A.* **93**, 2915 (1996).
- K. Diaz Gonzalez and A. Nieto, *FEBS Lett.* **361**, 255 (1995).
- A. Peri, E. Cordella-Miele, L. Miele, A. B. Mukherjee, *J. Clin. Invest.* **92**, 2099 (1993); A. Peri, N. Dubin, R. Dhanireddy, A. B. Mukherjee, *ibid.* **96**, 343 (1995).
- T. Kikukawa and A. B. Mukherjee, *Mol. Cell. Endocrinol.* **62**, 177 (1989); A. Aoki et al., *Mol. Hum. Reprod.* **2**, 489 (1996).
- P. J. Jackson, R. Turner, J. N. Keen, R. A. Brooksbank, E. H. Cooper, *J. Chromatogr.* **452**, 359 (1989).
- M. J. Beato, *J. Steroid Biochem.* **7**, 327 (1976); G. Singh et al., *Biochim. Biophys. Acta* **950**, 329 (1988); M. Gillener et al., *J. Steroid Biochem.* **31**, 27 (1988); M. A. Watson and T. P. Fleming, *Cancer Res.* **56**, 860 (1996).
- B. S. Chilton, S. K. Mani, D. W. Bullock, *Mol. Endocrinol.* **2**, 1169 (1988); G. W. Randall, J. C. Daniel Jr., B. S. Chilton, *J. Reprod. Fertil.* **91**, 249 (1991).
- S. M. Magdaleno et al., *Am. J. Physiol. Lung Cell Mol. Physiol.*, in press.
- A. B. Mukherjee, R. Ulane, A. K. Agrawal, *Am. J. Reprod. Immunol.* **2**, 135 (1982); D. C. Mukherjee, A. K. Agrawal, R. Manjunath, A. B. Mukherjee, *Science* **219**, 989 (1983); G. Vasanthakumar, R. Manjunath, A. B. Mukherjee, H. Warabi, E. Schiffmann, *Biochem. Pharmacol.* **37**, 389 (1988).
- Z. Zhang et al., *DNA Cell Biol.* **16**, 73 (1997).
- M. K. Ray, S. Magdaleno, B. W. O'Malley, F. J. DeMayo, *Biochem. Biophys. Res. Commun.* **197**, 163 (1993).
- A. Nagy, J. Rossant, R. Nagy, W. Abramow-Newerly, J. C. Roder, *Proc. Natl. Acad. Sci. U.S.A.* **90**, 8424 (1993).
- M. R. Capecchi, *Science* **244**, 1288 (1989); B. H. Koller and O. Smithies, *Annu. Rev. Immunol.* **10**, 705 (1992).
- An experimental protocol was approved by the institutional animal care and use committee. Total RNAs were isolated from different organs of UG^{+/+}, UG^{+/-}, and UG^{-/-} mice and reverse transcribed with mouse UG-specific primer, mPr (5'-ATC TTG CTT ACA CAG AGG ACT TG-3'). The PCR product was further amplified with primers mPI (5'-ATC GCC ATC ACA ATC ACT GT-3') and mPr. The PCR product was hybridized with an oligonucleotide probe, mPp (5'-ATC AGA GTC TGG TTA TGT GGC ATC C-3'), derived from exon-2 of the UG gene sequence. The primers and the probe used in mouse glyceraldehyde phosphate dehydrogenase (GAPDH) RT-PCR are as follows: mGAPDH-r (5'-GGC ATC GAA GGT GGA AGA GT-3'); mGAPDH-l (5'-ATG GCC TTC CGT GTT CCT AC-3'); and mGAPDH-p (5'-GAA GGT GGT GAA GCA GGC ATC TGA GG-3').
- Tissue lysates from the kidneys, liver, and lungs of UG^{+/+} and UG^{-/-} mice were prepared by homogenizing tissue samples in a buffer (10 mM tris-HCl, pH 7.5, 1% Triton X-100, 0.2% deoxycholate, 150 mM NaCl, 5 mM EDTA) containing 2 mM phenylmethylsulfonyl fluoride and 20 µg/ml each of aprotinin, leupeptin, and pepstatin A. The homogenates were centrifuged at 17,500g for 30 min at 4°C and immunoprecipitated as described [E. Harlow and D. Lane, *Antibodies: A Laboratory Manual* (Cold Spring Harbor Laboratory, Cold Spring Harbor, NY, ed. 1, 1988)] by incubating tissue lysates or plasma proteins (1 mg/ml) with rabbit antibody to murine Fn (anti-Fn) (1:100 dilution). Coimmunoprecipitation of purified murine Fn and recombinant human UG [G. Mantle et al., *J. Biol. Chem.* **267**, 20343 (1993)] was performed by incubating equimolar concentrations of Fn with UG in the presence of 10% glycerol, 50 mM tris-HCl, pH 7.5, 250 mM NaCl, and 4.3 mM sodium phosphate at 4°C for 1 hour, followed by the addition of anti-Fn (1:100 dilution). Equal amounts of extracted tissue proteins (30 µg) or immunoprecipitates were resolved either on 4 to 20% gradient or 6% SDS-polyacrylamide gels under reducing conditions, followed by protein immunoblotting with either anti-Fn (1:2000 dilution) or rabbit antibodies to murine UG (anti-UG) (1:2000 dilution).
- Tissues from UG^{-/-}, UG^{+/-}, and UG^{+/+} mice were fixed in Bouin's fluid or in 10% neutral-buffered formalin fixatives, embedded in paraffin, and sectioned at 4 to 6 µm. They were stained with hematoxylin and eosin (H and E). Selected tissues were stained by Masson's trichrome method for collagen detection, PTAH for fibrin, or Congo Red for amyloid protein. For immunohistochemical detection of UG and Fn, the Vectastain rabbit Elite ABC kit (Vector Laboratories) was used. The rabbit antibody (CyltIm-mune) to murine UG (mUG) was raised by using a synthetic peptide (Peptide Technologies) corresponding to mUG amino acid sequence Lys³⁰ to Thr⁵¹. The rabbit antibody to murine Fn (Gibco-BRL) was used at a dilution of 1:1000, and the antibody to UG was used at 1:500.
- A kidney from a UG^{-/-} mouse, with glomerular lesions, was fixed in formalin and embedded in epoxy resin. Thin sections stained with uranyl acetate and lead citrate were examined with an electron microscope. Photomicrographs were taken either at ×6000 or at ×60,000.
- Formalin-fixed tissue sections were used for immu-

- no fluorescence as described (5) with anti-Fn and fluorescein isothiocyanate (FITC)-conjugated goat antibody to rabbit IgG. Similarly, immunofluorescence studies with antibodies specific for Fn, collagens I and III, vitronectin, laminin, and osteopontin were also done. Epifluorescence was photographed with a Zeiss Axiophot microscope.
22. E. Ruoslahti, *Annu. Rev. Biochem.* **57**, 375 (1988); R. O. Hynes, *Fibronectins* (Springer-Verlag, New York, 1990); M. A. Chernousov, F. J. Fogarty, V. E. Koteliansky, D. F. Mosher, *J. Biol. Chem.* **266**, 10851 (1991); Q. Zhang, W. J. Chechovich, D. M. Peters, R. M. Albrecht, D. F. Mosher, *J. Cell Biol.* **127**, 1447 (1994); C. Wu, V. M. Kelvens, T. E. O'Toole, J. A. McDonald, M. H. Ginsberg, *Cell* **83**, 715 (1995); Q. Zhang and D. F. Mosher, *J. Biol. Chem.* **271**, 33284 (1996).
23. W. A. Border and E. Ruoslahti, *J. Clin. Invest.* **90**, 1 (1992).
24. Age-, sex-, and weight-matched UG^{+/+} (n = 3) and UG^{-/-} mice (n = 3) were killed and serum PLA₂ activities of each sample were measured in triplicate with a PLA₂-assay kit (Caymen Chemical) according to the instructions of the manufacturer. Protein concentrations in the sera were determined by Bradford assay (Bio-Rad), and specific activities of PLA₂ were determined.
25. Using 24-well plates coated with human Fn (hFn) (Collaborative Biomedical Products), we incubated 3 μl of ¹²⁵I-Fn (specific activity of 6 μCi/μg; ICN Biomedicals) in the absence and presence of either UG or Fn (10⁻¹² to 10⁻⁶ M) in 500 μl of Hanks' balanced salt solution (HBSS) at room temperature for 2 hours. SDS-PAGE and protein immunoblotting of all Fn with anti-UG failed to detect any UG contamination. The radiolabeled complex was washed twice with phosphate-buffered saline (PBS), solubilized in 1 N NaOH, and neutralized with 1 N HCl, and radioactivity was measured by a gamma counter. In a separate experiment ¹²⁵I-hFn (3 μl) was incubated with 20 μl (1 μg/μl) of mouse Fn in 40 μl of HBSS, pH 7.6, in the absence or presence of increasing concentrations of reduced UG (5 to 500 μg) at room temperature for 2 hours. The samples were cross-linked with 0.20 mM DSS at room temperature for 20 min, boiled in SDS sample buffer for 5 min, electrophoresed on a 4 to 20% gradient SDS-polyacrylamide gel, and autoradiographed. In another experiment, 15 μl of either denatured or nondenatured ¹²⁵I-collagen I (specific activity of 65.4 μCi/μg) was incubated with Fn in presence of reduced UG (250 μg), affinity cross-linked, electrophoresed, and autoradiographed.
26. Human Fn (500 μg/150 μl of PBS) was administered in the tail vein (27 of 2-month-old, ~22-g, UG^{+/+} and apparently healthy UG^{-/-} mice. Similarly, the control mice were injected with a mixture of 500 μg of hFn either with equimolar concentrations of UG or BSA in 150 μl of PBS. Twenty-four hours after the last injection, the mice were killed and various organs fixed in buffered formalin. Accumulation of hFn immunoreactivity in tissues was analyzed by immunofluorescence (6) with a monoclonal antibody to hFn (Gibco-BRL; clone 1) and FITC-conjugated rabbit antibody to mouse IgG (Cappel). In a separate experiment, UG^{+/+} mice were injected with 1 mg of Fn alone in 150 μl of PBS daily for three consecutive days.
27. E. Oh, M. Pierschbacher, E. Ruoslahti, *Proc. Natl. Acad. Sci. U.S.A.* **78**, 3218 (1981).
28. Z. Zhang *et al.*, unpublished results.
29. Fn matrix assembly and fibrillogenesis in cultured cells (CRL6336, American Type Culture Collection) were determined as described [D. F. Mosher, J. Sotile, C. Wu, J. A. McDonald, *Curr. Biol.* **4**, 810 (1992)].
30. G. Mazzucco, E. Maran, C. Rollino, G. Monga, *Hum. Pathol.* **23**, 63 (1992); E. H. Strom *et al.*, *Kidney Int.* **48**, 163 (1995); K. J. M. Assmann, R. A. P. Koene, J. F. M. Wetzels, *Am. J. Kidney Dis.* **25**, 781 (1995); O. Gempferle, J. Neuweiler, F. Reutter, F. Hidebrandt, R. Krapf, *ibid.* **28**, 668 (1996).
31. A Bam HI-Eco RI 3.2-kb DNA fragment containing exon-3 of 129/SVJ mouse UG gene (14) and its flanking sequences were subcloned into the corresponding site of the pPNW vector as described [K. Lei *et al.*, *Nature Genet.* **13**, 203 (1996)]. A 0.9-kb PCR-amplified fragment containing partial exon-2 and its flanking sequences with built-in Not I and Xho I sites were subcloned into the vector to generate the targeted construct pPNWUG. In pPNWUG, a 1.2-kb DNA fragment, including partial exon-2, was replaced with the PGK-*neo* cassette, disrupting the UG gene. Not I-linearized targeting construct DNA (25 μg) was electroporated into ES R1 cells. Chimeric mice were mated with C57BL/6 strain of mice, and germline transmission of the mutated UG allele was identified by PCR and Southern blot analyses of offspring tail DNA. The genotyping of progeny was carried out by PCR with a set of *neo*-specific primers, *neo*-L (5'-ATA CGC TTG ATC CGG CTA CCT GCC-3') and *neo*-R (5'-CAT TTG CAC TGC CGG TAG AAC TCC-3'), which yield a 667-base pair (bp) DNA fragment. A 304-bp DNA fragment was generated with a set of UG-specific primers, mUG-L (5'-ACA TCA TGA AGC TCA CAG GTA TGC-3') and mUG-R (5'-GTG TGC ACG GTT CAA GCT TGT AGT-3'), derived from the region of the UG gene that was replaced by the PGK-*neo* cassette. After an initial denaturing step (95°C for 2 min), 40 cycles of PCR were performed (94°C for 1 min, 58°C for 1.5 min, 72°C for 1 min) with a final step at 72°C for 10 min, by using a Perkin-Elmer 480 DNA thermal cyclor.
32. The contributions of G.C.K. and C.-J.Y. in delineating the mechanism of UG action should be considered equal. We thank A. Nagy, R. Nagy, and W. Abramow-Newerly for ES R1 cells; L. Miele for statistical analyses; L. Miele and G. Mantile-Selvaggi for facilitating recombinant UG production in *Escherichia coli*; A. Kulkarni, K. M. Yamada, J. Chou, I. Owens, S. W. Levin, J. DeB. Butler, K.-J. Lei, and C.-J. Pan for their assistance, discussions, and suggestions, and Syntex Research for gancyclovir. Supported in part by a USPHS grant (number HL47620 to F.D.).

15 January 1997; accepted 27 March 1997

A Cellular Cofactor for the Constitutive Transport Element of Type D Retrovirus

Hengli Tang, Guido M. Gaietta, Wolfgang H. Fischer, Mark H. Ellisman, Flossie Wong-Staal*

A human nuclear protein that specifically interacts with the constitutive transport element (CTE) of simian retrovirus was identified as adenosine 5'-triphosphate-dependent RNA helicase A. This protein could bind to functional CTE but not to inactive CTE mutants. The interaction of helicase A with CTE was distinct from previously described helicase activity of this protein. Helicase A shuttled from the nucleus to the cytoplasm in the presence of a transcription inhibitor or in cells transiently overexpressing CTE-containing RNA. In vivo colocalization of helicase A and CTE was observed in experiments that combined in situ hybridization and immunostaining. These results suggest that helicase A plays a role in the nuclear export of CTE-containing RNA.

Normal cellular mRNAs are exported from the nucleus as fully spliced RNA. However, retroviruses need to export partially spliced or unspliced RNA to the cytoplasm, both as templates for protein synthesis and as genomic RNA to be packaged in progeny virions. The complex retroviruses, including the human pathogenic retroviruses human T cell leukemia virus and human immunodeficiency virus (HIV), mediate this process through trans-acting proteins (Rex and Rev, respectively) that bind to their cognate RNA targets (RxRE and RRE, respectively). The simple retroviruses do not encode such trans-acting proteins but rather use cis-acting sequences that presumably interact directly with cellular nuclear export proteins. One example is the CTE of

type D retroviruses, which is able to functionally replace Rev or RRE in subgenomic constructs and infectious HIV clones (1, 2). Here we report the identification and characterization of a candidate for the cellular cofactor of CTE.

Wild-type and a nonfunctional mutant CTE (Δ CTE) were biotinylated and used in RNA selection experiments (3, 4). A 140-kD protein was reproducibly selected by wild-type but not by mutant CTE (Fig. 1A, lanes 1 and 2). Use of a panel of CTE deletion mutants revealed a complete correlation of CTE function [as determined in a chloramphenicol acetyltransferase (CAT) reporter assay (4)] and the ability to select the 140-kD protein (Table 1). We separated the 140-kD protein from other cellular proteins by SDS-polyacrylamide gel electrophoresis (SDS-PAGE) and excised it from a polyvinylidene difluoride (PVDF) membrane after blotting. We subjected tryptic peptides to microsequencing as described (5). Three independently sequenced internal peptides matched with three different parts of one protein in a BLAST homology search: human adenosine triphosphate (ATP)-dependent RNA helicase A, a DEAD-box helicase that belongs to the

H. Tang, Department of Biology, University of California, San Diego, La Jolla, CA 92093, USA.

G. Gaietta and M. H. Ellisman, Department of Neurosciences, and San Diego Microscopy Imaging Resource, University of California, San Diego, La Jolla, CA 92093, USA.

W. H. Fischer, Clayton Foundation Laboratories for Peptide Biology, Salk Institute, La Jolla, CA 92097, USA.

F. Wong-Staal, Department of Medicine and Biology, University of California, San Diego, La Jolla, CA 92093-0665, USA.

*To whom correspondence should be addressed.